University of
Strathclyde
Glasgow

Strathprints Institutional Repository

http://strathprints.strath.ac.uk/

Detailed analysis of hollow ions spectra from dense matter pumped by X-ray emission of relativistic laser plasma

S. B. Hansen, J. Colgan, A. Ya. Faenov, J. Abdallah Jr., S. A. Pikuz Jr., I. Yu. Skobelev, E. Wagenaars, N. Booth, O. Culfa, R. J. Dance, G. J. Tallents, R. G. Evans, R. J. Gray, T. Kaempfer, K. L. Lancaster, P. McKenna, A. K. Rossall, K. S. Schulze, I. Uschmann, A. G. Zhidkov, and N. C. Woolsey

---

Detailed analysis of hollow ions spectra from dense matter pumped by X-ray emission of relativistic laser plasma

S. B. Hansen,[1,a)] J. Colgan,[2] A. Ya. Faenov,[3,4,a)] J. Abdallah, Jr.,[2] S. A. Pikuz, Jr.,[3]
I. Yu. Skobelev,[3] E. Wagenaars,[5] N. Booth,[6] O. Culfa,[5] R. J. Dance,[5] G. J. Tallents,[5]
R. G. Evans,[7] R. J. Gray,[8] T. Kaempfer,[9] K. L. Lancaster,[6] P. McKenna,[8] A. K. Rossall,[5]
K. S. Schulze,[9] I. Uschmann,[9,10] A. G. Zhidkov,[11] and N. C. Woolsey[5]

[1]*Sandia National Laboratories, Albuquerque, New Mexico 87123, USA*
[2]*Theoretical Division, Los Alamos National Laboratory, Los Alamos, New Mexico 87545, USA*
[3]*Joint Institute for High Temperatures, Russian Academy of Sciences, Moscow 125412, Russia*
[4]*Quantum Beam Science Directorate, Japan Atomic Energy Agency, Kyoto 619-0215, Japan*
[5]*York Plasma Institute, Department of Physics, University of York, York YO10 5DD, United Kingdom*
[6]*Central Laser Facility, STFC Rutherford Appleton Laboratory, Didcot OX11 0QX, United Kingdom*
[7]*Department of Physics, Imperial College, London SW7 2AZ, United Kingdom*
[8]*SUPA, Department of Physics, University of Strathclyde, Glasgow G4 ONG, United Kingdom*
[9]*Helmholtzinstitut Jena, Jena D-07743, Germany*
[10]*Institut für Optik und Quantenelektronic, Friedrich-Schiller-Universität Jena, Max-Wien Platz 1,
Jena, D-07743, Germany*
[11]*PPC Osaka University and JST, CREST, Osaka 565-0871, Japan*

X-ray emission from hollow ions offers new diagnostic opportunities for dense, strongly coupled plasma. We present extended modeling of the x-ray emission spectrum reported by Colgan *et al.* [Phys. Rev. Lett. **110**, 125001 (2013)] based on two collisional-radiative codes: the hybrid-structure Spectroscopic Collisional-Radiative Atomic Model (SCRAM) and the mixed-unresolved transition arrays (MUTA) ATOMIC model. We show that both accuracy and completeness in the modeled energy level structure are critical for reliable diagnostics, investigate how emission changes with different treatments of ionization potential depression, and discuss two approaches to handling the extensive structure required for hollow-ion models with many multiply excited configurations. © *2014 AIP Publishing LLC*. [http://dx.doi.org/10.1063/1.4865227]

I. INTRODUCTION

The X-ray emission from plasmas produced by low-contrast optical or infrared laser pulses with picosecond and/or femtosecond duration has been actively investigated in the last two decades. Generally, the main spectral features of X-rays emission from this wide range of incident laser parameters have been found to be similar to that previously observed in experiments with long (nanosecond) laser pulses with strong resonance line emission from closed-shell ions, well-resolved red-side satellite emission, and in the case of intense laser pulses ($>10^{17}$ W/cm^2), cold characteristic lines generated by non-thermal electrons. Recently, however, experiments performed with high-contrast ($\sim 10^{10}$) femtosecond lasers[1,2] were shown to produce qualitatively different emission spectra, which in addition to relatively weak resonance lines and practically unresolved satellites also exhibited complex, quasi-continuous emission.

In Refs. 1–4, it was shown that this new type of observed spectra can be interpreted only by taking into account the radiation emitted by multiply charged hollow ions of KK type (i.e., ions with an completely empty K-shell; see the notation of hollow ions in, for example, Ref. 5) in a near-solid-density plasma. Transitions of this kind have also been observed in experiments in which ion beams,[6–15] synchrotron radiation,[16,17] or X-ray free electron laser (XFEL) beams[18,19] interact with a solid target. Similar emission patterns for multiply charged ions apparently were first observed from laser plasmas in the spectra emitted from surface plasmas produced by a nanosecond pulse at the Naval Research Laboratory's NIKE laser facility.[20]

Like conventional X-ray emission spectra, hollow-ion emission has the potential to be a powerful plasma diagnostic. For strongly-coupled, non-ideal plasmas such as those in the challenging regime of Warm Dense Matter, hollow-ion spectra have the distinct advantage of being relatively insensitive to the coupling effects of the plasma environment, since the transitions take place between deep inner shells of the ion. Hollow ion emission is also useful for diagnostics of hot dense plasma, where the large optical depths of conventional emission lines limit their diagnostic utility.

Producing a significant population of hollow ions in plasma requires a mechanism which efficiently removes electrons from the inner shell while retaining significant population in outer shells, but such selective excitation is obtained only under very particular conditions. In general, ionization can occur upon collision of an ion with an electron, ion, or photon.

In ion-ion collisions, both non-resonant ionization by the Coulomb field of the incident ion and the resonant charge-exchange are possible. The first process can be neglected in plasma, since the ion impact ionization cross sections are large only for ultra high energy ions, which are at present efficiently

---

a)Authors to whom correspondence should be addressed. Electronic addresses: sbhanse@sandia.gov and anatolyf@hotmail.com

produced only in accelerators.[21] It should be noted, however, that the first observations of the spectra of hollow atoms (hollow atom is a special case of a hollow ion with zero total charge) were done in accelerator experiments.[6] The second mechanism, resonant charge exchange with preferential population of outer shells, can produce different states of hollow ions if the interaction of ions with significantly different multiplicities occurs. This may be done, for example, when laser plasma expands into a residual gas.

Most often, the ionization processes in the plasma occur due to electron impact. In this case, the electron energy must be larger than the ionization energy of the inner shell, but not so large as is required for ionization by ions. Indeed, for ions with a charge of 10, electrons with energies of a few keV could be sufficient for inner-shell ionization. It is well known[22–28] that in plasma produced by femtosecond or picosecond, laser pulses with intensities higher than 10^{16} W/cm^2 such electrons are generated very efficiently and can impact the plasma emission, particularly by generating characteristic inner-shell lines such as Kα. However, since hot electrons also remove outer-shell electrons, they are not very effective in producing hollow ions. Indeed, the rates of electron impact ionization scale approximately with n^3, where n is the principal quantum number of the ionizing electrons. It follows that hot electrons preferentially (by almost an order of magnitude) ionize L-shell electrons rather than K-shell. Thus during ion collisions with hot electrons, hollow ions are formed, but their abundance is far lower than the usual abundance of ions. This conclusion is practically independent of whether hot electrons are monoenergetic (electron beam) or have a thermal distribution. For example, in Ref. 29 it was shown that although the relative populations of hollow ions increase rapidly with increasing laser pulse intensity (by increasing the fraction of hot electrons), even for laser intensity of I $= 10^{18}$ W/cm^2 the hollow ion population is only about 1% relative to states with only one inner-shell vacancy.

The situation is quite different in the case of X-ray photoionization, since the photoionization cross section is approximately proportional to n^{-5}, i.e., a photon incident on an ion will preferentially remove an electron from the innermost shell that is energetically allowed. Currently, the process of hollow ion production by X-rays is of particular importance due to the advent of multiple high-power X-ray lasers such as: transient–collisional, based on plasma pumping by visible lasers[30–33] and the free-electron lasers.[18,19,34,35] In contrast to the interaction of the optical laser radiation with the matter, the absorption of X-ray radiation is directly related to the formation of hollow ions. Recall that during the action of the optical laser pulse on matter, the bulk of its energy goes into heating the first encountered free electrons. And only then due to electron-ion collisions is the energy converted into internal energy of the ions (via impact ionization and the formation of multiply charged ions) and later on into their kinetic energy. During the absorption of X-ray photon, by contrast, a big part of the energy goes directly to the internal energy by the formation of autoionizing states and hollow ions, and then only part of it will be transferred to the free electrons of the plasma following auto-ionization. In this case, the

conditions of the resulting plasma are strongly dependent on the ratio of X-ray laser photon energies and the ionization potentials of the different atomic shells of the target material.

Bright X-ray emission from a plasma may also generate hollow ions by their own plasma radiation. This could occur in situations where the plasma has strong temperature inhomogeneity. For example, the radiation arising in a central hot area of laser spot could create hollow ions in a cold periphery region, where the electron temperature is not sufficient to ionize the outer shells of the ion.[36]

Another very important X-ray source that can produce hollow ions has recently been experimentally realized in Refs. 1 and 37. It was demonstrated that during the interaction of optical laser radiation with an intensity of $> 10^{20}$ W/cm^2 with thin foils, the interaction of laser photons with oscillating electrons, due to effects of radiation dominant regime,[38–41] produced X-rays with an intensity of $\sim 10^{19}$ W/cm^2. These are broadband radiation sources with intensities that exceed those from monochromatic and coherent XFEL.

Given current trends in laser-matter interaction studies, requiring the use of more and more powerful lasers to produce ultra-intense X-rays, hollow-ion plasmas may soon become very common and the spectra of hollow ions will be one of the most informative diagnostics of such plasma. It is thus essential to pursue systematic theoretical and experimental studies on the spectroscopy of hollow ions in X-ray-pumped plasma sources. The objectives of these studies should be:

(1) To establish the role of the various configurations and processes, including plasma effects such as line broadening and ionization potential depression (IPD) in the formation of hollow ions and the emission spectrum of the plasma.
(2) To provide calculations of the dependence of the emission spectrum of the macroscopic parameters of the plasma, its density, temperature and hot electron characteristics, and the local radiation field.
(3) To determine the hollow ion spectra dependences on laser parameters including the intensity of the laser pulse, its duration, contrast, focal spot dimensions, as well as the dependence on target materials and geometries.

All these will help developing methods of X-ray spectral diagnostics of warm and hot dense plasma.

In this paper, two independent models are used to provide a detail theoretical study of the role of the various configurations and processes in the formation of hollow-ion emission spectra, and the model results were compared with the experimentally observed Al spectra from thin targets irradiated by the Vulcan laser as reported in Refs. 1 and 37. In particular, modeling descriptions and calculations are developed to explain the spectral features and widths measured between 7.8 and 8.2 Å, which result from transitions in KL hollow ions

II. EXPERIMENTS

The experiments were done at the Vulcan Petawatt (PW) facility at the Rutherford Appleton Laboratory.[42] The

laser pulse of ~ 1.0 ps duration and 10^9 amplified spontaneous emission (ASE) contrast several nanoseconds ahead of the peak of the laser pulse delivered up to 160 J on the target. The laser radiation was focused with an f/3 off-axis parabola to a focal spot of 8 μm diameter (FWHM) containing approximately 30% of the energy, achieving a maximum intensity of 3×10^{20} W/cm^2. The horizontally polarized laser beam was incident on target at 40° from the target surface normal.

The spectra shown in Fig. 1 were measured by means of focusing spectrometer with spatial resolution (FSSR) spectrometer[43] equipped with spherically bent mica crystal (lattice spacing $2d = 19.9376$ Å, radius of curvature of $R = 150$ mm). The crystal was aligned to operate at $m = 2$ order of reflection to record K-shell emission spectra of multicharged Al ions in 7.0–8.4 Å of wavelength range. The FSSR spectral resolving power was approximately 5000. The spectrometer observed the laser-irradiated front surface of the target at an angle of 45° to the target surface normal. Spectra were recorded on Kodak Industrex AA400 film protected against exposure to visible light using two layers of 1 μm thick polypropylene $(C_3H_6)_n$ coated with 0.2 μm Al, or with 25 μm thick beryllium foil. Background fogging and crystal fluorescence due to intense fast electrons were limited using a pair of 0.5 T neodymium-iron-boron permanent magnets that formed a slit 10 mm wide in front of the crystal.

Pure Al targets of 20 μm and 1.5 μm thickness foils were examined. For the case of the "thin" aluminum target and full available laser energy of 160 J (thin black line in Fig. 1) intense, broad spectral line groups dominate the spectrum and occur between the resonance line positions (accepted wavelengths[44] for aluminum Ly$_\alpha$ (7.17 Å) and He$_\alpha$ (7.76 Å) resonance lines together with the K$_\alpha$ line (8.34 Å) are indicated by the vertical dotted lines). The most compelling explanation for these spectral lines groups is emission due to transitions in KK and KL hollow ions. The spectral line group positions do not match known transitions for any

FIG. 1. Experimental X-ray spectra[1] of 1.5 μm thickness Al foils excited by Vulcan PW ~ 1 ps laser pulses: Black line—target irradiated by 160 J laser pulse. Blue line—target irradiated by 64 J laser pulse. The red line indicates the best correspondence with measured data and was obtained using the ATOMIC code at the following conditions: Planckian radiation field of Tr = 3 keV, with a bulk electron temperature (Te) of 55 eV and electron density (Ne) of 3×10^{23} cm^{-3}, with ion number density of 5.9×10^{22} cm^{-3}, and a small fraction (5%) of the electrons with a temperature 5 keV. The plots are offset for convenience.

ionization stage of aluminum that has populated inner shells. Indeed, hollow-ion spectral line emission is anticipated in the spectral range between 7.17 and 7.76 Å, i.e., between the Ly$_\alpha$ and He$_\alpha$ resonance lines and below 8.34 Å, i.e., on the short wavelength side of the K$_\alpha$ line. We conclude that in the "thin" targets a large population of hollow ions is created, and the radiation from these hollow ions dominates in the spectral range observed.

The reduction of the laser pulse energy from 160 to 64 J, as the laser intensity on the "thin" target decreases from 3×10^{20} W/cm^2 to $\sim 1 \times 10^{20}$ W/cm^2, leads to other remarkable changes in the spectra (thin blue line in Fig. 1). The intensity of the spectral features between the resonance lines, i.e., the hollow atom emission, drops and the spectra mostly contain of He$_\alpha$ and Ly$_\alpha$ lines with some conventional satellites. These observations underscore the importance of the fact that the optical laser intensity must exceed 10^{20} W/cm^2 in order to create conditions that result in copious KK and KL hollow atom generation. In Refs. 1 and 37, X-ray spectra were modeled by performing atomic kinetics calculations using the ATOMIC code.[45,46] As could be seen from comparison experimental and modeled spectra in Fig. 1, theory could do rather well reproducing the observed emission through a complex treatment of double K-shell holes hollow ions in atomic structure and spectral synthesis calculations. However, the model did not fully reproduce the spectra for single K-shell holes (KL hollow ions and ordinary satellites), which occur in the spectral range of 7.8–8.4 A. Sections III and IV show how additions to the structure included in the models and modifications to the broadening can help resolve the outstanding discrepancies and investigate the effects of using different IPD models.

III. MODELING

The ATOMIC model used to produce the emission spectrum shown in Fig. 1 was described in detail in Refs. 1 and 37. Here, we build on that work and test the convergence of our calculations with respect to the number of configurations included. We find that model convergence requires up to 7 electrons excited from the K and L shells into the M shell. Such a model, which is somewhat larger than that used previously,[1,36,37] produces thousands of configurations per ion stage, for a total of over 21000 non-relativistic configurations. Our atomic collision calculations are performed within the configuration-average approximation to generate all the required excitation and ionization cross sections. All transitions are treated on an equal footing, i.e., no averaging of data is used.

We also use the mixed-unresolved transitional arrays (MUTA) approach to include the effects of detailed lines and configuration interaction in the emission spectrum.[47] This approach retains all the lines within a transition array if the number of lines within the array is less than 10^6. Such lines are computed in fine structure with the inclusion of intermediate-coupling (i.e., interactions such as spin-orbit mixing are included between levels arising from the same configuration). Calculations that include full configuration-interaction (CI) for all of the configurations included in our model
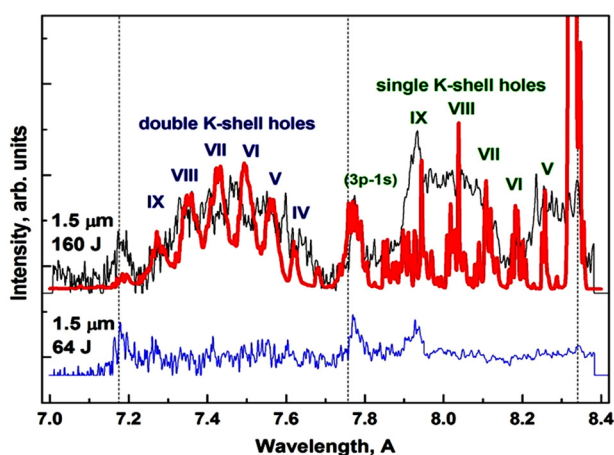
become computationally prohibitive. However, we have been able to perform calculations that include full configuration-interaction for a restricted set of configurations. Such calculations were made for those configurations that are important for the KL emission between 7.8 and 8.2 A. These calculations find that the emission arising from a full CI calculation is very similar to the emission from a MUTA calculation, and in particular, the KL line positions and widths predicted from each calculation are quite close. An illustration of the good agreement between a full CI calculation and a MUTA calculation is shown in Fig. 2 for a single ion stage (Al^{7+}). Such a study provides confidence in the accuracy of the MUTA approach to predicting emission spectra. Figure 2 also shows the KL transitions from C-like Al calculated using relativistic and non-relativistic unresolved transitional arrays (UTAs), which have much more limited CI: the "ATOMIC UTA" calculation includes the effects of broadening that mimics the intermediate coupling within the non-relativistic configurations, and the relativistic unresolved transitional arrays (RUTA) calculation includes only intermediate coupling within the relativistic configurations. Note that the ATOMIC RUTA calculation can be considered deficient in that it does not include the coupling between the relativistic configurations (that arise from the same non-relativistic configuration); this coupling would be automatically included in the non-relativistic UTA broadening. These approximations lead to broader features and, in the case of the RUTAs, significant shifts in the central wavelengths.

The ATOMIC calculations shown in this work include collisional broadening of the lines (which dominates other broadening mechanisms due to the high electron density) and the effects of IPD via the Stewart-Pyatt (SP) model.[48] Since our calculations retain a large number of explicit configurations and utilize the detailed line structure provided through the MUTA approach, the solution of the collisional-radiative rate equations and the generation of the emission spectrum can be computationally intensive.

The second model considered here is the hybrid-structure Spectroscopic Collisional-Radiative Atomic Model (SCRAM),[49] which is based on fine-structure-level data from
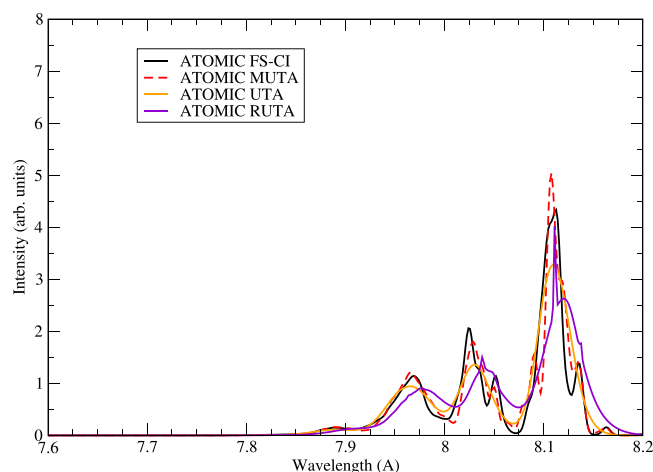

FIG. 2. KL emission from the Al^{7+} ion for a restricted set of configurations. We compare a model computed using full configuration-interaction within the atomic structure to that computed using the MUTA approach that is used for the complete calculations presented in Secs. III and IV.

the Flexible Atomic Code (FAC)[50] for single excitations of valence- and inner-shell electrons from the ground configurations and for selected KL and KK hollow-core states of all ions. These states are supplemented by additional multiply excited and high-n relativistic configurations and UTAs from FAC with configuration-interaction corrections.[51] Statistical completeness is ensured by the addition of screened hydrogenic superconfigurations for many-times excited states.[52–55] An iterative process systematically excites electrons from the valence and inner shells of the previous iteration's superconfigurations until the population in the most highly excited superconfigurations in each ion is less than some threshold value (typically about 1%).

For example, calculation of the C-like ion stage begins with the $(1)^2(2)^4$ superconfiguration, which is initially expanded to $(1)^2(2)^3(n)^1$ and $(1)^1(2)^4(n)^1$. Similar structure is generated for other ions, with the maximum principal quantum number set by neutral ion-sphere IPD ($n_{max} \sim 4$–5 for the range of ions and similar to SP in the present conditions). We also considered the modified Ecker-Kroll IPD model recently advocated in Ref. 19, which destroys the 3d (but not 3s or 3p) orbitals in C-like Al. If the population in the singly excited configurations is more than 1% of the total ion population after the full non-LTE system is solved, then each $(1)^2(2)^3(n)^1$ state generates a set of $(1)^2(2)^2(n)^1(n')^1$ and $(1)^1(2)^3(n)^1(n')^1$ states, and each $(1)^1(2)^4(n)^1$ state generates a set of $(1)^1(2)^3(n)^1(n')^1$ states and (KK hollow-ion) $(2)^4(n)^1(n')^1$ states. Duplicate states are eliminated and convergence is again tested. In the extreme conditions created by the experiment described above, convergence typically requires up to nine iterations of excitation for the most complex ions, resulting in more than 200 distinct superconfigurations in the C-like ion alone, with excitations up to $(5)^6$ using ion-sphere IPD and a total statistical weight for the ion of more than 10^9. Treating the entire set of energy levels for all ions with fine structure detail would be computationally prohibitive.

Once convergence is reached in the screened hydrogenic model, selected hydrogenic superconfigurations are replaced by more accurate and detailed FAC-based fine structure and relativistic configurations as described in Ref. 54, the rate equations for the resulting hybrid-structure model are solved, and emission and absorption spectra are calculated. The spectra include fine-structure lines for Heα, Lyα, and some KL and KK satellites along with relativistic UTAs and transitions from the superconfigurations for additional KL and KK satellites. The n-n' transitions from the superconfigurations are split into nlj transitions based on ground-state structure calculations,[56] corrected by comparison with the more accurate FAC data, and shifted following the screened hydrogenic calculations to account for multiple excitations. All lines are broadened by collisions, Stark, and opacity effects. Collisions dominate the broadening for the conventional satellites. In addition, FAC UTA widths are included along with widths based on the shell variances of inactive electrons; these widths dominate the KK emission in the SCRAM calculations.

We emphasize that while the fine structure lines and FAC-based relativistic UTAs in the hybrid-structure model

are fairly accurate, the accuracy of the transitions from the superconfigurations is much more limited, as illustrated in the comparison of SCRAM with the more accurate ATOMIC/MUTA model that is presented below. However, the SCRAM calculations are much more efficient, completing in minutes rather than days. To produce approximations for the hollow-ion emission, it is necessary establish a suitable compromise which enables the construction of a statistically complete and computationally tractable model. An alternative approach to modeling complex transition arrays given in Ref. 57 offers a promising path to increasing accuracy in Kα emission while maintaining tractability.

Figure 3 illustrates the dependences of the calculated emission spectra from SCRAM for solid-density Al at various electron and radiation temperatures with and without hot electrons. Although calculations are shown for only one ion density (6×10^{22} ions/cm^3), the model can produce moderate hollow-ion emission intensities for densities down to 10% of solid if the radiation field is diluted by the same fraction. At much lower densities where three-body processes do not dominate the recombination, it becomes impossible to significantly populate hollow ion states while maintaining multiple L-shell electrons.

At the near-solid densities maintained in a thin-foil target under intense, high-contrast optical laser irradiation, the charge state distribution is largely determined by the thermal electron temperature Te, shifting from near Ne-like at Te = 10 eV to B-like around Te = 50 eV, regardless of radiation field or hot electrons. With neither hot electrons nor a strong radiation field, there would be minimal K-shell radiation from Al ions at these low temperatures. Including a significant radiation field leads to a profound increase in the intensity of hollow ion emission but leads to only small changes in the charge state distribution and the intensities of
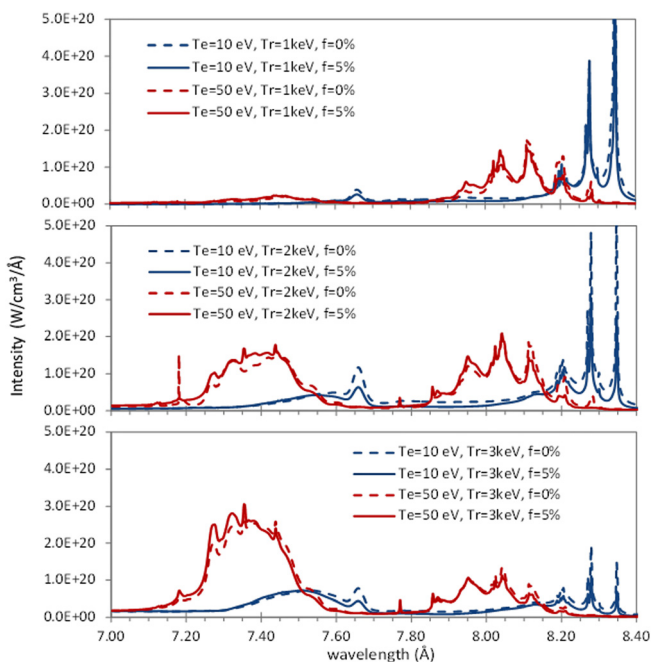
the conventional satellite and KL hollow ion emission. While hot electrons can excite KL emission in the absence of high Tr, the impact of even a 5% fraction of hot electrons in the presence of a significant radiation field is modest. These trends are very similar to those predicted by the ATOMIC modeling presented in Ref. 37.

Figure 4 shows the emission of solid-density Al with Te = 50 eV, Tr = 2 keV, and f = 5% broken down by ion from ATOMIC with SP IPD and from SCRAM with two different approximations for the IPD. In the ATOMIC and SCRAM calculations with SP or neutral ion-sphere IPD, the most intense emission feature from each ion occurs at a higher energy than the "fundamental" transition energy associated with single or double excitations. These "secondary" features arise from transitions among multiply excited states with high-lying spectator electrons, indicating significant population in the multiply excited states. Indeed, the fraction of population in each ion that lies in the ground superconfiguration is only ~10% at these conditions, as listed in the legend of the central plot. The differences between SCRAM and ATOMIC in the internal structures of the features from each ion and even their central wavelength positions, particularly for secondary emission features, reflect the more extensive detailed atomic structure included in the ATOMIC model. We also note that the collisional-radiative modeling from ATOMIC and SCRAM predict slightly different ionization balances, with SCRAM being more ionized by about one charge state.

FIG. 3. Calculated optically thin emission from the SCRAM model showing dependence of emission on Te, Tr, and hot electron fraction, assuming a 5 keV Maxwellian hot electron distribution.
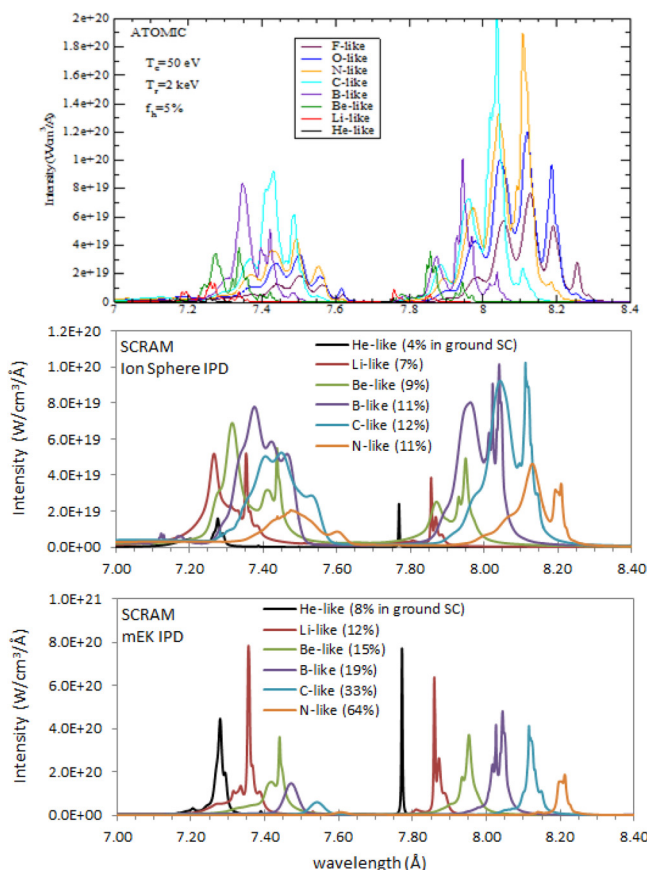

FIG. 4. Emission broken down by ion from ATOMIC with Stewart-Pyatt IPD (top) and SCRAM with Ion Sphere (middle), and modified Ecker-Kroll (bottom) IPD. All calculations use Te = 50 eV, Tr = 2 keV, and f = 5%.

This difference is reflected in the different intensities of the emission contributions from the various Al ions and is primarily due to the slightly different treatments of pressure ionization. The effects of pressure ionization also manifest in the relative intensities of the features from each ion: in SCRAM, where the orbitals are gradually destroyed under pressure ionization by a reduction of their statistical weights, emission from the multiply excited states contributes somewhat less than in ATOMIC, where the full statistical weight is retained until the orbital is completely destroyed.

The sensitivity of the models to IPD and pressure ionization is underscored in the bottom plot of Fig. 4 by using a modified Ecker-Kroll (mEK) model for the IPD[19,58] in SCRAM, which results in the destruction of many of the high-n, highly excited states. This shifts the charge state distribution to even more highly charged ions, increases the fraction of population in the ground superconfigurations, and decreases or eliminates the relative intensities of the secondary emission features in proportion to the destruction of highly excited states. The mEK IPD model has been invoked to explain the unexpected early onset of fluorescence emission with increasing incident XFEL energies on solid Al at Linac Coherent Light Source (SLAC) with Te $\sim$ 100 eV.[18,19] The SCFLY code,[55] which uses screened hydrogenic levels for kinetics and Dirac-Fock relativistic UTAs for emission spectra, provided very good agreement with the LCLS data using mEK and much poorer agreement using SP. And while recent measurements of resonant Kβ emission from compressed plasmas with Te $\sim$ 600 eV created using the Orion laser[59] indicate that the M-shell electrons of H- and He-like Al persist at densities up to $\sim$6 g/cc, in agreement with ion-sphere IPD but not mEK, an extended IPD model proposed by Crowley[60] agrees with both the Orion and LCLS experiments and predicts IPD values for the present conditions that are closer to mEK than to ion sphere. However, the narrow features arising from the fine-structure states in SCRAM that dominate the KK emission when the mEK IPD is used are not observed in the quasi-continuous measured KK emission spectrum, providing some indication that the M-shell is not completely destroyed. Since the ion density is not independently known in the present experiments, the measured emission cannot be used to discriminate among IPD models; future measurements extending to lower wavelengths could be of critical importance in determining whether the M-shell survives in similar plasmas.

IV. DIAGNOSTICS

Acknowledging the uncertainty in the IPD and the limitations of the hybrid-structure approach in terms of exact line positions of emission from multiply excited states, we diagnose the plasma conditions with SCRAM for the measured experimental emission from the 160 J pulse incident on the 1.5 μm Al target by seeking a "gestalt" fit that reproduces the gross features of the time-and space-integrated data. This fit, which uses ion sphere IPD, is presented in the upper panel of Fig. 5. The emission comes from three almost equally weighted regions, all assumed to be at solid density (similar fits could be obtained using mEK IPD at a density
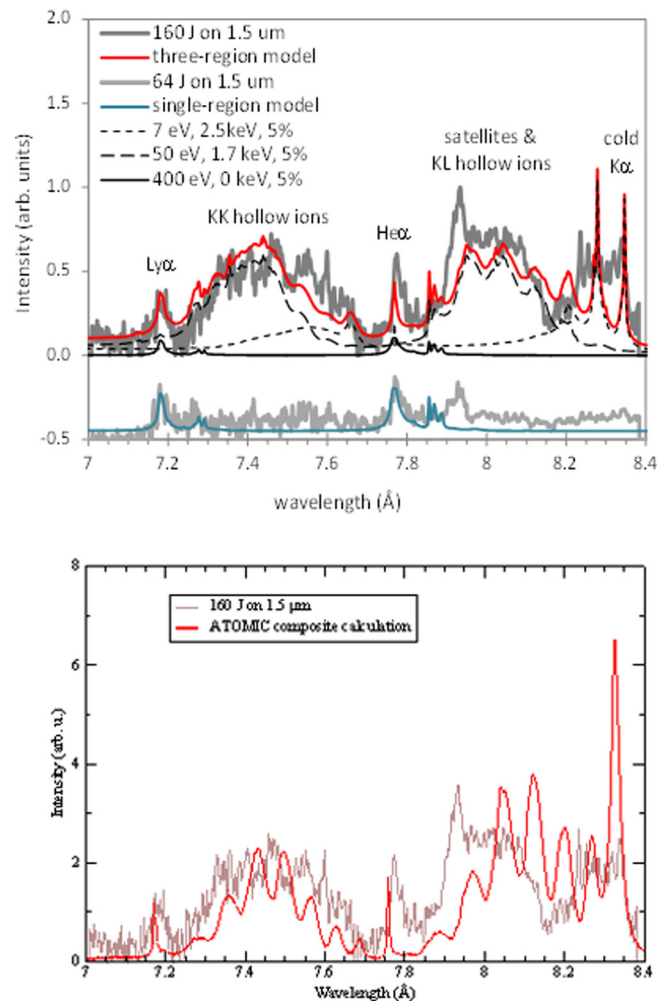

FIG. 5. Upper panel: SCRAM model fits to experimental spectra at two different laser intensities, lower panel: ATOMIC comparison to the experimental spectra for the 160 J experiment.

nearer 1 g/cc, which is still high enough to support significant population in the multiply excited states). The first region includes the entire depth of the 1.5-μm target at a relatively cold thermal temperature (7 eV), with 5% hot electrons and a 2.5 keV radiation field. This region contributes the cold Kα and the KL and KK emission from near-Ne-like ions. The second region has a higher thermal temperature of 50 eV and a lower radiation temperature of 1.7 keV, and contributes the KL and KK emission from mid-L-shell ions. Finally, there is a hotter region with Te $\sim$400 eV and 5% hot electrons with no radiation field that includes only about a tenth of the original target thickness, but with a larger weighting factor that could be attributable to a larger area or longer duration. Self-consistent opacity effects are included in all three regions using the escape factor approximation. The measured emission from the 64 J laser pulse incident on a 1.5 μm target is also shown in Fig. 5 (upper panel). This spectrum does not have significant hollow-ion emission and is reasonably well fit by the high-temperature region with no radiation field, although it would be fit almost as well with any Tr < 1 keV. This is consistent with the mechanism for radiation production proposed in Ref. 1, which predicts a near-linear scaling of the radiation temperature with the laser energy.

The lower panel of Figure 5 presents the new ATOMIC calculations in comparison with the experimental spectrum obtained from the 160 J laser incident on the 1.5 μm target. These are also composite calculations including contributions from multiple plasma regions. The only difference from the SCRAM calculations is that the ATOMIC calculations use a bulk electron temperature of 40 eV rather than 50 eV in the second region in order to obtain better agreement with the observed emission spectrum. Further fine-tuning of the precise conditions used in the ATOMIC calculations may marginally improve the agreement with experiment.

The new ATOMIC modeling shows significantly improved agreement with experiment for the KL spectra (between 7.8 and 8.2 Å), whereas the comparison of the KK spectra (between 7.2 and 7.7 Å) is similar to that obtained previously.[1] The ATOMIC calculations still predict an emission spectrum with lines that are not as broad as found experimentally. Collisional broadening is the dominant broadening mechanism in the ATOMIC calculations and we note that the ATOMIC MUTA calculations do not require any UTA broadening prescriptions. It is possible that other broadening mechanisms, not included in the ATOMIC model, are contributing in this case, or that perhaps radiation transport influences the spectrum in a way not properly accounted for by the simple escape factor approach used in ATOMIC.

There remains a feature around 7.93 Å in both experimental spectra, coinciding with the conventional satellite feature from Be-like Al that is not reproduced by either of the models. Although Be-like Al is a closed-shell ion, it is difficult to find plasma conditions that produce Be-like emission without also producing emission from its neighboring ions, and the prominence of the feature remains unexplained by both ATOMIC and SCRAM.

V. CONCLUSIONS

Hollow-ion emission from radiation-dominated hot, dense plasmas provides a new opportunity for diagnosing high-intensity x-ray radiation fields. However, constructing adequate non-LTE atomic models remains a challenge, since there remains uncertainty in the IPD at these conditions, configuration interaction plays a significant role in the structure of the emission, and multiply excited states with many holes in both valence and inner shells can lead to enormous structural and computational complexity. We know of no atomic kinetics model that systematically and self-consistently accounts for all these effects.

We have presented two approaches to modeling emission spectra from atoms with extensive structure: first, the ATOMIC model, which uses a mixture of fine structure levels and UTAs, is shown to provide highly accurate line positions and relative intensities. A complete accounting of the highly excited states is shown to be possible, although computationally intensive. The statistically complete hybrid-structure SCRAM model has highly accurate treatments of selected conventional resonance and satellite lines and can ensure completeness by systematically adding

superconfigurations until the population converges. However, the emission features arising from transitions between these superconfigurations are not very accurate. Despite their shortcomings, both models can provide reasonable general agreement with the measured hollow-ion emission spectra collected using the high-contrast Vulcan laser on a thin Al foil.

We have shown that increasing model completeness by including additional configurations significantly improves the agreement between the modeled and measured spectra as compared with previous modeling published in Ref. 1 and shown in Fig. 1 above. Additional work remains to be done to balance accuracy and completeness in the model calculations, to find reliable representations for the configuration and collisional broadening effects, and to better understand the role of IPD in radiation-dominated hot dense plasmas, where calculations become sensitive to the interplay between pressure ionization, which reduces the available state space, and the radiation field, which makes many-times-excited states energetically accessible.

[1]J. Colgan, J. Abdallah, Jr., A. Ya. Faenov, S. A. Pikuz, E. Wagenaars, N. Booth, O. Culfa, R. J. Dance, R. G. Evans, R. J. Gray, T. Kaempfer, K. L. Lancaster, P. McKenna, A. L. Rossall, I. Yu. Skobelev, K. S. Schulze, I. Uschmann, A. G. Zhidkov, and N. C. Woolsey, Phys. Rev. Lett. **110**, 125001 (2013).
[2]A. Ya. Faenov, J. Abdallah, Jr., R. E. H. Clark, J. Cohen, R. P. Johnson, G. A. Kyrala, A. I. Magunov, T. A. Pikuz, I. Yu. Skobelev, and M. D. Wilke, Proc. SPIE **3157**, 10 (1997); A. M. Urnov, J. Dubau, A. Ya. Faenov, T. A. Pikuz, I. Yu. Skobelev, J. Abdallah, Jr., R. E. H. Clark, J. Cohen, R. P. Johnson, G. A. Kyrala, M. D. Wilke, and A. L. Osterheld, JETP Lett. **67**, 489 (1998); A. Maksimchuk, M. Nantel, G. Ma, S. Gu, C. Y. Cote, D. Umstadter, S. A. Pikuz, I. Yu. Skobelev, and A. Ya. Faenov, J. Quant. Spectrosc. Radiat. Transfer **65**, 367 (2000).
[3]A. Ya. Faenov, A. I. Magunov, T. A. Pikuz, I. Yu. Skobelev, S. A. Pikuz, A. M. Urnov, J. Abdallah, R. E. H. Clark, J. Cohen, R. P. Johnson, G. A. Kyrala, M. D. Wilke, A. Maksimchuk, D. Umstadter, N. Nantel, R. Doron, E. Behar, P. Mandelbaum, J. J. Schwob, J. Dubau, F. B. Rosmej, and A. L. Osterheld, Phys. Scr. **T80**, 536 (1999).
[4]F. B. Rosmej, U. N. Funk, M. Geissel, D. H. H. Hofmann, A. Tausehwitz, A. Ya. Faenov, T. A. Pikuz, I. Yu. Skobelev, F. Flora, S. Bollanti, P. Di Lazzaro, T. Letardi, A. Grilli, L. Palladino, A. Reale, A. Scafati, L. Reale, T. Auguste, P. D'Oliveira, S. Hulin, P. Monot, A. Maksimchuk, S. A. Pikuz, D. Umstadter, M. Nanatel, R. Bock, M. Dornik, M. Stetter, S.

Stoewe, V. Yakushev, M. Kulish, and N. Shilkin, J. Quant. Spectrosc. Radiat. Transfer **65**, 477 (2000).

[5] I. Yu. Skobelev, A. Ya. Faenov, T. A. Pikuz, and V. E. Fortov, Phys. Usp. **55**, 47 (2012).

[6] J. P. Briand, L. de Billy, P. Charles, S. Essabaa, P. Briand, R. Geller, J. P. Desclaux, S. Bliman, and C. Ristori, Phys. Rev. Lett. **65**, 159 (1990).

[7] J. Bailey, A. L. Carlson, G. Chandler, M. S. Derzon, R. J. Dukart, B. A. Hammel, D. J. Johnson, T. R. Lockner, J. Maenchen, E. J. McGuire, T. A. Mehlhorn, W. E. Nelson, L. E. Ruggles, W. A. Stygar, and D. F. Wenger, Lasers Part. Beams **8**, 555 (1990).

[8] J. Limburg, S. Schippers, R. Hoekstra, R. Morgenstern, H. Kurz, F. Aumayr, and H. P. Winter, Phys. Rev. Lett. **75**, 217 (1995).

[9] J.-P. Briand, G. Giardino, G. Borsoni, M. Froment, M. Eddrief, C. Sebenne, S. Bardin, D. Schneider, J. Jin, H. Khemliche, Z. Xie, and M. Prior, Phys. Rev. A **54**, 4136 (1996).

[10] S. Ninomiya, Y. Yamazaki, F. Koike, H. Masuda, T. Azuma, K. Komaki, and M. Sekiguchi, Phys. Rev. Lett. **78**, 4557 (1997).

[11] J.-P. Briand, D. Schneider, S. Bardin, H. Khemliche, J. Jin, Z. Xie, and M. Prior, Phys. Rev. A **55**, 3947 (1997).

[12] H. Winter and F. Aumayr, J. Phys. B **32**, R39 (1999).

[13] T. Schenkel, A. V. Hamza, A. V. Barnes, and D. H. Schneider, Prog. Surf. Sci. **61**, 23 (1999).

[14] S. J. McMahon, A. P. Kavanagh, H. Watanabe, J. Sun, M. Tona, N. Nakamura, S. Ohtani, and F. Currell, Phys. Rev. A **83**, 022901 (2011).

[15] J. Rzadkiewicz, A. Gojska, O. Rosmej, M. Polasik, and K. Slabkowska, Phys. Rev. A **82**, 012703 (2010).

[16] R. Diamant, S. Huotari, K. Hamalainen, C. C. Kao, and M. Deutsch, Phys. Rev. Lett. **84**, 3278 (2000); Phys. Rev. A **62**, 052519 (2000).

[17] R. Diamant, S. Huotari, K. Hamalainen, R. Sharon, C. C. Kao, and M. Deutsch, Phys. Rev. A **63**, 022508 (2001); Phys. Rev. Lett. **91**, 193001 (2003).

[18] S. M. Vinko, O. Ciricosta, B. I. Cho, K. Engelhorn, H.-K. Chung, C. R. D. Brown, T. Burian, J. Chalupský, R. W. Falcone, C. Graves, V. Hájková, A. Higginbotham, L. Juha, J. Krzywinski, H. J. Lee, M. Messerschmidt, C. D. Murphy, Y. Ping, A. Scherz, W. Schlotter, S. Toleikis, J. J. Turner, L. Vysin, T. Wang, B. Wu, U. Zastrau, D. Zhu, R. W. Lee, P. A. Heimann, B. Nagler, and J. S. Wark, Nature **482**, 59 (2012).

[19] O. Ciricosta, S. M. Vinko, H.-K. Chung, B.-I. Cho, C. R. D. Brown, T. Burian, J. Chalupsky, K. Engelhorn, R. W. Falcone, C. Graves, V. Hájková, A. Higginbotham, L. Juha, J. Krzywinski, H. J. Lee, M. Messerschmidt, C. D. Murphy, Y. Ping, D. S. Rackstraw, A. Scherz, W. Schlotter, S. Toleikis, J. J. Turner, L. Vysin, T. Wang, B. Wu, U. Zastrau, D. Zhu, R. W. Lee, P. Heimann, B. Nagler, and J. S. Wark, Phys. Rev. Lett. **109**, 065002 (2012).

[20] Y. Aglitsky, T. Lehecka, A. Deniz, J. Hardgrove, J. Seely, C. Brown, U. Feldman, C. Pawley, K. Gerber, S. Bodner, S. Obenschain, R. Lehmberg, E. McLean, M. Pronko, J. Sethian, J. Stamper, A. Schmitt, C. Sullivan, G. Holland, and M. Laming, Phys. Plasmas **3**, 3438 (1996).

[21] V. E. Fortov, Phys. Usp. **52**, 615 (2009).

[22] J. Abdallah, Jr., A. Ya. Faenov, I. Yu. Skobelev, A. I. Magunov, T. A. Pikuz, T. Auguste, P. D'Oliveira, S. Hulin, and P. Monot, Phys. Rev. A **63**, 032706 (2001).

[23] A. G. Zhidkov, A. Sasaki, I. Fukumoto, T. Tajima, T. Auguste, P. D'Olivera, S. Hulin, P. Monot, A. Ya. Faenov, T. A. Pikuz, and I. Yu. Skobelev, Phys. Plasmas **8**, 3718 (2001).

[24] S. Hansen, A. S. Shlyaptseva, A. Y. Faenov, I. Y. Skobelev, A. I. Magunov, T. A. Pikuz, F. Blasco, F. Dorchies, C. Stenz, F. Salin, T. Auguste, S. Dobosz, P. Monot, P. D'Oliveira, S. Hulin, U. I. Safronova, and K. B. Fournier, Phys. Rev. E **66**, 046412 (2002).

[25] J. Abdallah, Jr., A. G. Csanak, Y. Fukuda, Y. Akahane, M. Aoyama, N. Inoue, H. Ueda, K. Yamakawa, A. Ya. Faenov, A. I. Magunov, T. A. Pikuz, and I. Yu. Skobelev, Phys. Rev. A **68**, 063201 (2003).

[26] M. E. Sherrill, J. Abdallah, Jr., G. Csanak, E. S. Dodd, Y. Fukuda, Y. Akahane, M. Aoyama, N. Inoue, H. Ueda, K. Yamakawa, A. Ya. Faenov, A. I. Magnov, T. A. Pikuz, and I. Yu. Skobelev, Phys. Rev. E **73**, 066404 (2006).

[27] K. B. Fournier, A. Ya. Faenov, T. A. Pikuz, I. Yu. Skobelev, V. S. Belyaev, V. I. Vinogradov, A. S. Kyrilov, A. P. Matafonov, I. Bellucci, S. Martelluci, G. Petrocelli, T. Auguste, S. Hulin, P. Monot, and P. D'Oliveira, Phys. Rev. E **67**, 016402 (2003).

[28] O. Culfa, G. J. Tallents, E. Wagenaars, C. P. Ridgers, R. J. Dance, A. K. Rossall, R. J. Gray, P. McKenna, C. D. R. Brown, S. F. James, D. J. Hoarty, N. Booth, A. P. L. Robinson, K. L. Lancaster, S. A. Pikuz, A. Ya.

Faenov, T. Kampfer, K. S. Schulze, I. Uschmann, and N. C. Woolsey, "Hot electron production in laser solid interactions with a controlled pre pulse," Plasma Phys. (submitted).

[29] K. Moribayashi, A. Sasaki, and A. Zhidkov, Phys. Scr. **T92**, 185 (2001).

[30] R. C. Elton, *X-ray Lasers* (Academic, 1990).

[31] J. J. Rocca, "Table-top soft X-ray lasers," Rev. Sci. Instrum. **70**, 3799 (1999).

[32] H. Daido, "Review of soft X-ray laser researches and developments," Rep. Prog. Phys. **65**, 1513 (2002).

[33] S. Suckewer and P. Jaegle, "X-ray lasers: past, present, future," Laser Phys. Lett. **6**, 411 (2009).

[34] P. Emma, R. Akre, J. Arthur, R. Bionta, C. Bostedt, J. Bozek, A. Brachmann, P. Bucksbaum, R. Coffee, F.-J. Decker, Y. Ding, D. Dowell, S. Edstrom, A. Fisher, J. Frisch, S. Gilevich, J. Hastings, G. Hays, Ph. Hering, Z. Huang, R. Iverson, H. Loos, M. Messerschmidt, A. Miahnahri, S. Moeller, H.-D. Nuhn, G. Pile, D. Ratner, J. Rzepiela, D. Schultz, T. Smith, P. Stefan, H. Tompkins, J. Turner, J. Welch, W. White, J. Wu, G. Yocky, and J. Galayda, Nature Photon. **4**, 641 (2010).

[35] T. Ishikawa, H. Aoyagi, T. Asaka, Y. Asano, N. Azumi, T. Bizen, H. Ego, K. Fukami, T. Fukui, Y. Furukawa, S. Goto, H. Hanaki, T. Hara, T. Hasegawa, T. Hatsui, A. Higashiya, T. Hirono, N. Hosoda, M. Ishii, T. Inagaki, Y. Inubushi, T. Itoga, Y. Joti, M. Kago, T. Kameshima, H. Kimura, Y. Kirihara, A. Kiyomichi, T. Kobayashi, C. Kondo, T. Kudo, H. Maesaka, X. M. Maréchal, T. Masuda, S. Matsubara, T. Matsumoto, T. Matsushita, S. Matsui, M. Nagasono, N. Nariyama, H. Ohashi, T. Ohata, T. Ohshima, S. Ono, Y. Otake, C. Saji, T. Sakurai, T. Sato, K. Sawada, T. Seike, K. Shirasawa, T. Sugimoto, S. Suzuki, S. Takahashi, H. Takebe, K. Takeshita, K. Tamasaku, H. Tanaka, R. Tanaka, T. Tanaka, T. Togashi, K. Togawa, A. Tokuhisa, H. Tomizawa, K. Tono, S. Wu, M. Yabashi, M. Yamaga, A. Yamashita, K. Yanagida, C. Zhang, T. Shintake, H. Kitamura, and N. Kumagai, Nature Photon. **6**, 540 (2012).

[36] J. Colgan, J. Abdallah, Jr., C. J. Fontes, D. P. Kilcrease, J. Dunn, M. Purvis, and R. W. Lee, High Energy Density Phys. **6**, 295 (2010).

[37] S. A. Pikuz, A. Ya. Faenov, J. Colgan, R. J. Dance, J. Abdalla, E. Wagenaars, N. Booth, O. Culfa, R. G. Evans, R. J. Gray, T. Kaempfer, K. L. Lancaster, P. McKenna, A. L. Rossall, I. Yu. Skobelev, K. S. Schulze, I. Uschmann, A. G. Zhidkov, and N. C. Woolsey, High Energy Density Phys. **9**, 560 (2013).

[38] A. Zhidkov, J. Koga, A. Sasaki, and M. Uesaka, Phys. Rev. Lett. **88**, 185002 (2002).

[39] T. Nakamura, J. K. Koga, T. Zh. Esirkepov, M. Kando, G. Korn, and S. V. Bulanov, Phys. Rev. Lett. **108**, 195001 (2012).

[40] C. P. Ridgers, C. S. Brady, R. Duclous, J. G. Kirk, K. Bennett, T. D. Arber, A. P. L. Robinson, and A. R. Bell, Phys. Rev. Lett. **108**, 165006 (2012).

[41] R. R. Pandit and Y. Sentoku, Phys. Plasmas **19**, 073304 (2012).

[42] C. N. Danson, P. A. Brummitt, R. J. Clarke, J. L. Collier, B. Fell, A. J. Frackiewicz, S. Hawkes, C. Hernandez-Gomez, P. Holligan, M. H. R. Hutchinson, A. Kidd, W. J. Lester, I. O. Musgrave, D. Neely, D. R. Neville, P. A. Norreys, D. A. Pepler, C. J. Reason, W. Shaikh, T. B. Winstone, R. W. W. Wyatt, and B. E. Wyborn, Laser Part. Beams **23**, 87 (2005); I. Musgrave, W. Shaikh, M. Galimberti, A. Boyle, C. Hernandez-Gomez, K. Lancaster, and R. Heathcote, Appl. Opt. **49**, 6558 (2010).

[43] A. Ya. Faenov, S. A. Pikuz, A. I. Erko, B. A. Bryunetkin, V. M. Dyakin, G. V. Ivanenkov, A. R. Mingaleev, T. A. Pikuz, V. M. Romanova, and T. A. Shelkovenko, Phys. Scr. **50**, 333 (1994).

[44] See http:\\spectr-w3.snz.ru for atomic constants mutlicharged ions.

[45] N. H. Magee, J. Abdallah, J. Colgan, P. Hakel, D. P. Kilcrease, S. Mazevet, M. Sherrill, C. Fontes, and H. L. Zhang, AIP Conf. Proc. **730**, 168–179 (2004).

[46] J. Colgan, J. Abdallah, Jr., A. Ya. Faenov, T. A. Pikuz, I. Yu. Skobelev, Y. Fukuda, Y. Hayashi, A. Pirozhkov, K. Kawase, T. Shimomura, H. Kiriyama, Y. Kato, S. V. Bulanov, and M. Kando, High Energy Density Phys. **7**, 77 (2011).

[47] S. Mazevet and J. Abdallah, Jr., J. Phys. B **39**, 3419 (2006).

[48] J. C. Stewart and K. D. Pyatt, Jr., Astrophys. J. **144**, 1203 (1966).

[49] S. B. Hansen, J. Bauche, C. Bauche-Arnoult, and M. F. Gu, High Energy Density Phys. **3**, 109 (2007).

[50] M. F. Gu, Astrophys. J. **582**, 1241 (2003).

[51] S. B. Hansen, Can. J. Phys. **89**, 633 (2011).

[52] H.-K. Chung, M. H. Chen, W. L. Morgan, Y. Ralchenko, and R. W. Lee, High Energy Density Phys. **1**, 3 (2005).

[53]H. A. Scott and S. B. Hansen, High Energy Density Phys. **6**, 39 (2010).

[54]S. B. Hansen, J. Bauche, and C. Bauche-Arnoult, High Energy Density Phys. **7**, 27 (2011).

[55]H.-K. Chung, M. H. Chen, and R. W. Lee, High Energy Density Phys. **3**, 57 (2007).

[56]D. A. Liberman, J. R. Albritton, B. G. Wilson, and W. E. Alley, Phys. Rev. A **50**, 171 (1994).

[57]C. A. Iglesias and V. Sonnad, High Energy Density Phys. **8**, 154 (2012).

[58]T. R. Preston, S. M. Vinko, O. Ciricosta, H.-K. Chung, R. W. Lee, and J. S. Wark, High Energy Density Phys. **9**, 258 (2013).

[59]D. J. Hoarty, P. Allan, S. F. James, C. R. D. Brown, L. M. R. Hobbs, M. P. Hill, J. W. O. Harris, J. Morton, M. G. Brookes, R. Shepherd, J. Dunn, H. Chen, E. Von Marley, P. Beiersdorfer, H. K. Chung, R. W. Lee, G. Brown, and J. Emig, Phys. Rev. Lett. **110**, 265003 (2013).

[60]B. J. B. Crowley, "Continuum lowering – a new perspective," e-print arXiv:1309.1456.